Preliminary slope mass movements suceptibility mapping using LIDAR DEM

Michel Jaboyedoff
Institute of Risk Analysis – University of Lausanne, Lausanne, Switzerland
Andrea Pedrazzini, Pascal Horton, Alexandre Loye & Ivan Surace
Institute of Risk Analysis – University of Lausanne, Lausanne, Switzerland

ABSTRACT
Potential slope movements affecting the Canton of Vaud (3200 km^2), Switzerland, have been studied by means of DEM-based analysis and geological data. The goal of the study was to develop and apply different methods in order to provide a fast overview of potential events related to slope mass movement at regional scale. This paper presents an overview of the methods and discusses the advantage and the limitation of a DEM-based approach.

RÉSUMÉ
Une étude de susceptibilité aux mouvements de versant, basée sur l'analyse du modèle numérique de terrain (MNT) a été effectuée en Suisse dans le canton de Vaud (3200 km^2). L'objectif de cette étude était de développer et d'appliquer des méthodes rapides permettant d'avoir une vue d'ensemble des zones potentiellement touchées par les mouvements de versants. Les différentes méthodes ainsi que les avantages et limitations d'une approche basée sur l'analyse d'un MNT sont discutées.

1 INTRODUCTION

Regional susceptibility maps aim to provide a fast overview of potential events related to slope mass movement at regional scale. This consists of a preliminary hazard mapping of slope movements over an entire territory in order to assess whether an area is potentially endangered or not by slope movements like landslide, shallow landslide, debris flow and rockfall. Such maps do not give any information on the intensity and the frequency of occurrence of the slope movements. They only indicate the hazard locations at 1:25,000 map resolution. This kind of map belongs to the first step of the working process leading toward detailed local danger maps (Lateltin, 1997). Susceptibility maps of the canton of Vaud (Switzerland) were obtained using DEM-based analysis. This paper introduces an overview of the methodologies applied for the different slope processes.

2 GEOGRAPHICAL AND GEOLOGICAL SETTING

The susceptibility mapping was performed on the entire territory of the canton of Vaud (3200 km^2), western Switzerland. The geology can be divided into three main regions (Trümpy, 1980) (Figure 1):

- The northwestern region is located within the Jura chain. Its elevation ranges from 400 m to approx. 2000 m a.s.l.. This area is composed of folded and thrusted Mesozoic and Tertiary carbonates platform series, in a thin skin tectonic style.
- The middle part belongs to the Swiss Molasse Plateau. It corresponds to the foreland basin of Oligo-Miocene age. The rocks are mostly detritic from shales to conglomerates. The topography is hilly with, cliffs made of competent sandstones in some limited places or steep slopes resulting from fluvial erosion.
- The southeast area belongs to the Alpine region mostly in the Prealps. The morphology is first shaped by glacial erosion and reworked by fluvial erosion processes and slope mass movements. It presents a steep and rugged topography ranging from 400 to more than 3000 m. The lithological outcrops are mainly limestone, dolomites, marls, evaporites and shales. They are strongly controlling the type of slope movements. They were deposited in several different Mesozoic and Cenozoic basins.

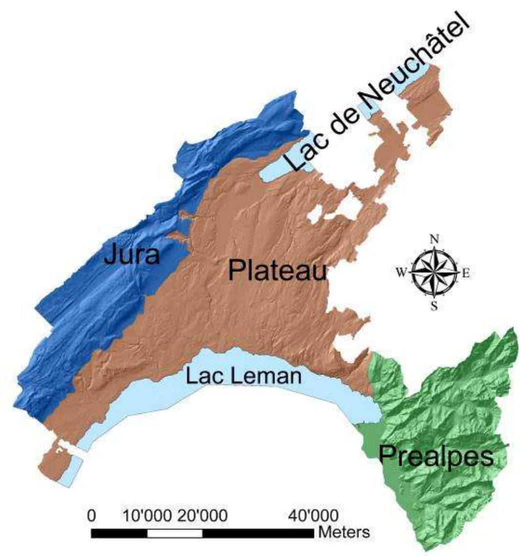

Figure 1: The canton Vaud could be divided in three distinct geological areas, characterized by a different lithology and a different tectonic history *(MNT-MO, © 2005 SIT).*

3 LANDSLIDE INVENTORY AND SUSCEPTIBILITY

3.1 Method

The method focused on the use of GIS tools and GIS Data (i.e. LiDAR-DEM of 1m x 1m cell size). The potential instabilities were identified by means of a systematic approach over the 3200 km^2 of the canton of Vaud, based on LiDAR-DEM analysis, information provided from the 1:25,000 geological maps as well as orthophotos. The validation of the results was based on a review of geological data, field observations and comparison with available historical inventories (Noverraz, 1995).

3.1.1 Updating the known instabilities with LiDAR-DEM

A landslides inventory was performed using a detailed investigation of the 1:25,000 topographic map and local knowledge was performed during the DUTI program (DUTI - EPFL 1985, NOVERRAZ 1995). Landslides were also extracted from geological maps. The landslide limits of the prior inventories were corrected following morphological evidence visible on the LiDAR-DEM hillshade and on the orthophotos. In the same way, new unstable areas were added to the landslide inventory map (Figure 2).

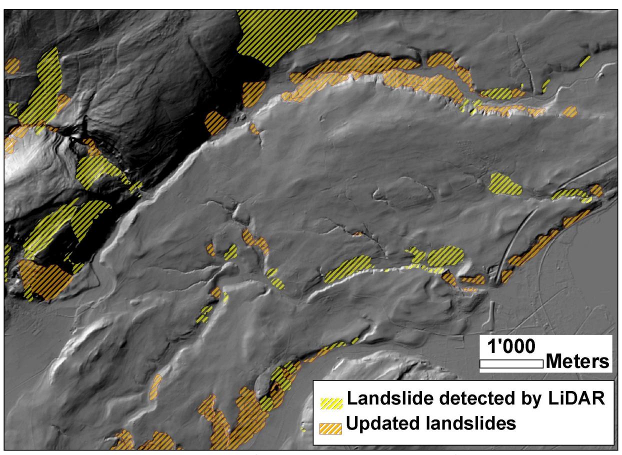

Figure 2: Example of the updating of the landslide susceptibility hazard map based on previous studies (Noverraz, 1995) and completed according to the morpho-structural analysis of LiDAR-DEM data *(MNT-MO, © 2005 SIT).*

3.1.2 Mapping the potential landslide prone areas

A map of the potential landslide areas was obtained by analyzing visually the LiDAR-DEM hillshade 2D and its 3D visualization simultaneously (Ardizzone et al., 2007). Such fine-scale morphological topographic analysis is a relevant approach for delineating potential landslides. According to a systematic approach based on morphological features (slope failures, scars, deposits, sagging) all kinds of topographic irregularities (slope statistics, etc.) were taken as evidence to delineate current and ancient landslide prone areas. Moreover, this approach was associated with the analysis of the 1:25'000 geological maps (www.swisstopo.ch), using the sensitivity of lithologies to landsliding, structural elements such as fault systems and tectonic lines. The slopes at rivers edges were also considered because of the effect of enhanced erosion in such a context (distortion of watercourses, occurrence of natural dams, etc.) and were therefore used as criterion to detect landslide activity. Then, the landslide susceptibility was subdivided in three categories from proven landslides (clear geomorphologic signatures) to zones that possess one or more criteria susceptible to contain landslides, but without any clear features (Figure 3). The three main susceptibility classes were described as follow:

Class 1: Zone characterized by the occurrence of landslides detected by a typical and complete set of morphological landslide features or based on previous inventories.

Class 2: Zone characterized by the occurrence of possible landslides deduced by some of the morphological evidence but which cannot be verified without a detailed field work.

Classes 3: *3a)* areas characterized by an important fluvial erosion. *3b)* areas showing a rugged topography (depression, scars, etc.). *3c)* areas characterized by a mean slope value between 18°-37°, which define a range of slope suitable to develop landslides (Van Westen et al, 1997).

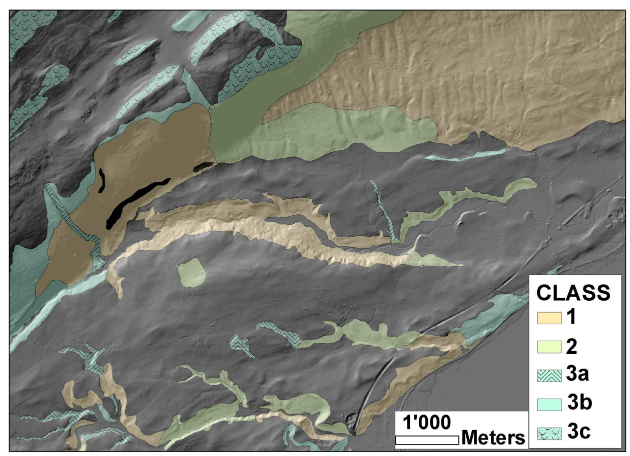

Figure 3: Close up of the landslide prone areas map based on DEM, orthophotos and geological map analysis. Each class corresponds to different morphological evidence and to different types of processes *(MNT-MO, © 2005 SIT).*

3.2 Creation of a GIS database

All these information related to the landslide susceptibility classes were stored in a GIS database and form an interactive landslides susceptibility map all over the territory, which consist of a complete description of information (distinctive morphological sign, class, etc.).

These characteristics enable an overview of the state of knowledge of the landslide prone areas.

3.3 Restriction in DEM interpretation

The limiting factor in interpreting LiDAR-DEM hillshade 2D and its 3D visualization depends principally to the data artifacts. They are mostly related to the occurrence of locally very dense vegetation cover or occurrence of clouds during the data acquisition as well as some steep rugged topography that truncates the laser signal during the data acquisition. Displaying hillshade can have some kind of shading effects as well, which creates inaccurate or even incorrect morpho-structural features.

4 SHALLOW LANDSLIDES

To assess the potential extension of shallow slope instability induced by heavy rainfall, the SINMAP method (Pack et al, 1998) was used. This GIS-based approach allows a rapid and uniform slope stability evaluation through a large territory.

4.1 Methodology

The SINMAP (Stability INdex MAPping) methodology is based on the infinite slope stability model (Montgomery and Dietrich, 1994) coupled with a steady state hydrological model, where computed depth of saturated soil must be sufficient to sustain a lateral discharge proportional to the specific catchment area (Pack et al, 1998). SINMAP allows entering variables uncertainties through the specification of lower and upper bounds for hydrological and geotechnical parameters. These introduce a probabilistic approach in the calculation of the factor of safety that allows to propose different possible scenarios. The derived dimensionless susceptibility index (SI) is given by Pack et al, 1998 (eq. 1):

$$SI = \frac{C' + \cos\theta\left[1 - \min\left(\frac{Ra}{T\sin\theta}, 1\right) r\right]\tan\phi}{\sin\theta\cos\theta} \qquad [1]$$

Where C' = dimensionless cohesion coefficient, θ = slope angle, Φ = friction angle, r= water to soil density ratio, a = specific catchment area, R/T = ratio corresponding to the steady state recharge relative to the effective rainfall quantity and the soil transmissivity.

4.2 Application to the canton of Vaud territory

The input data set of SINMAP consists of the DEM and a few parameters quantifying the hydrological and geotechnical conditions. In our study, due to the large area to be mapped, the LiDAR DEM was re-sampled in a DEM of 15m x 15m cell size. For the same reason, the study area was divided into three main zones corresponding to the 3 main geological conditions. The geotechnical parameters were estimated for each lithology of the 1:25000 geological maps (www.swisstopo.ch) based on literature data (Salciarini et al., 2006).

The T (Transmissivity) parameter was derived from the hydraulic conductivity (minimal and maximal) of the different lithologies. The R (Recharge) parameter is more difficult to calculate. Hence, in our study, it was assumed to be the effective precipitation for 24 hours rainfall with a return period of 100 years. These values have been chosen in order to give a maximal extension of the potential unstable area for rare event situations.

The model calibration was performed based on pre-existing inventory maps (Noverraz, 1995) and orthophotos observations. According to the goal of the susceptibility mapping project, the results of the SINMAP analysis were reclassified in a single susceptibility class containing pixels having a minimal SI lower than 1.

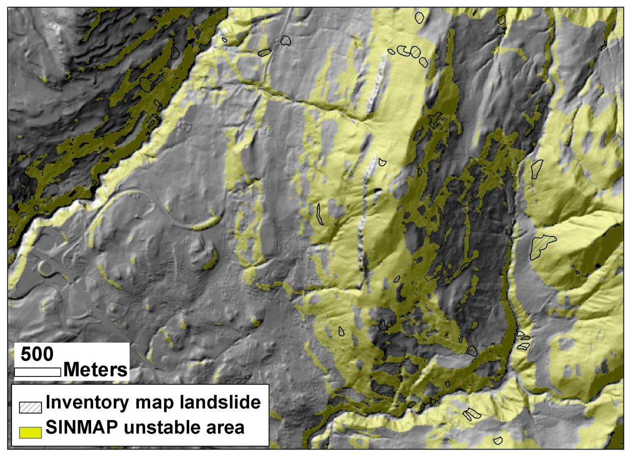

Figure 4: Close up of the shallow landslide susceptibility map, showing the good agreement with the inventoried shallow landslide. *SWISSIMAGE © 2004 swisstopo (DV012716)*

4.3 Results analysis

The comparison between the SINMAP results and the inventory landslide map shows that 78% of the inventoried landslides are contained in the predicted unstable zone. In general, 85% of inventoried landslides are found in a buffer of 50 m around the predicted unstable areas. The main differences between SINMAP results and the inventory map are found in the Jura region where the particular hydrological system (mainly karstic) makes the application of SINMAP model more difficult.

Compared to the total surface of the study area, the SINMAP analysis shows that 18% (576 km^2) of the canton of Vaud can be potentially affected by shallow landslides. The most susceptible region is the alpine region were the susceptible area increases to 55% of the overall surface.

5 DEBRIS FLOWS

The Alps contain numerous potential debris flows; so potential threats exist and must be considered. Process-based mechanical modeling of debris flows at a regional scale is difficult because of the complexity of the phenomenon and the variability of controlling factors. Therefore, a new simple model has been developed for a regional debris flow susceptibility assessment. The objective of this model is to allow a transparent algorithm choice and an easy customization of the method.

5.1 Methodology

The methodology involves a two step process. First, the debris flow sources were identified through different geological, morphological and hydrological criterial. Then, these sources were propagated and spread through a probabilistic and energetic approach on the basis of a Digital Elevation Model (DEM) with a map resolution of 10 m. The source volumes were not taken into account, due to impossible large scale rapid assessments and due to the significant mass changes occurring through deposition and erosion (Iverson *et al.* 2001), which is excessively difficult to estimate. The Matlab® environment was chosen for its optimized matrices data management and its large build-in libraries.

5.2 Source area identification

According to Rickenmann and Zimmermann (1993) and Takahashi (1981), three criteria in a critical combination are relevant for a debris flow initiation: sediment availability, water input and slope gradient.

For each criterion, a grid is generated containing three possible values for each cell: possible source – excluded – ignored. The possible source option means that according to the selected criterion, the cell is a potential source area. The ignored option means that there is no evidence if the cell is a source or not, so that no decision is fixed. The excluded option means that the cell cannot be a debris flow source area. By combining the grids established for the different criteria, a cell is selected as a source area if it was at least identified once as a possible source but never classified as excluded.

5.2.1 Slope

Most debris flows occur from terrain with a slope higher than 15° (Rickenmann and Zimmermann 1993; Takahashi 1981). Some initiation thresholds of other factors can be expressed in function of the slope angle, the lithology and the contributive area.

5.2.2 Curvature

Another potential morphological characteristic is the curvature as debris flows are found where curvature is concave (Delmonaco *et al.* 2003). To allow an identification of gullies, the plan curvature, which is perpendicular to the steepest slope, was considered.

5.2.3 Hydrology

The upslope contributing area is considered as a characteristic of water input (Erskine *et al.* 2006). On the basis of the calculated flow accumulation, by use of the D∞ algorithm (Tarboton 1997), the cells with a contributing area less than 1 ha were not considered as potential sources. A detection of the sources on the remaining cells was done through a threshold relationship with the slope.

Based on Rickenmann and Zimmermann (1993) observations of the 1987 debris flows in Switzerland, we established a new threshold limit that is more conservative than proposed earlier by other authors (eq. 2):

$$\begin{cases} \tan\,\beta_{lim} = 0.31\cdot S_{UA}^{-0.15} & \text{if } S_{UA} < 2.5\text{km}^2 \\ \tan\,\beta_{lim} = 0.26 & \text{if } S_{UA} \geq 2.5\text{km}^2 \end{cases} \qquad [2]$$

where tan β_{lim} = slope gradient and S_{UA} = surface of the upslope contributing area.

5.2.4 Lithology

The lithology was taken into account by means of a litho-geotechnical map that contains uniform information about outcropping formations for the whole study area. This so-called “geotype” map was established by the Swiss Federal Institute of Technology (EPFL) based on the Swiss Atlas of Geological 1:25’000 maps (www.swisstopo.ch). The selected lithologies are debris flow prone rocks (marl, slate, siltstone) and slope deposits.

5.2.5 Land use

Land use enables the removal of certain inaccurate sources that are located in built-up areas or that are man-made infrastructures. Rock outcrops were also excluded from potential sources, but forested areas were selected, because debris flows can be observed in forests, and because the protective effect of trees can be removed by a fire or a cut.

5.2.6 Criteria compilation

The sources were determined by compiling the various results from each dataset listed previously. The results were verified by orthophoto analysis and by rapid field survey.

5.3 Spreading area assessment

The debris flow spreading was estimated by two types of algorithms: the first ones are called flow direction algorithms and rule the path that the debris flow will follow; the second ones determine the runout distance. These two rules are used all along the path, from the source spreading initiation downstream to the end.

The flow can go from one cell to its eight neighbors. The direction of maximum probability of propagation is dependent on the slope angle and on the probability of lateral spreading in all directions; this allows an integration of the notion of inertia (Holmgren, 1994; Quinn *et al.* 1991; Claessens *et al.*, 2005; Gamma, 2000). Some conditions were defined so that there is always at least one cell in which the flow can run. The sum of the probabilities over all neighbors is equal to one.

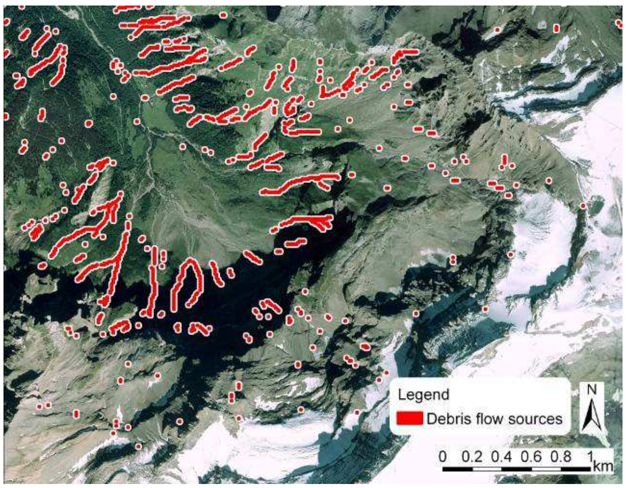

Figure 5: Identified potential debris flow sources for the Les Diablerets region (Switzerland) *SWISSIMAGE © 2004 swisstopo (DV012716).*

The runout distance was defined using a unit energy budget (eq. 3), a basic friction angle and a maximum velocity. It was assumed that the mass slides, loses energy by friction and acquires kinetic energy (difference between loss by friction and potential energy) by transforming potential energy into kinetic energy. This approach does not aim to represent exact physical processes, but to remain realistic.

$$E_{kin}^{i} = E_{kin}^{i-1} + \Delta E_{pot}^{i} - E_{loss}^{i} \quad [3]$$

where i = time step, E_{kin} = kinetic energy, ΔE_{pot} = change in potential energy and E_{loss} = constant loss.

If the velocity is over a threshold, it is not possible to increase the kinetic energy. The maximum threshold aims to limit the debris flow energy to reasonable values. The chosen threshold is a maximum velocity of 15 $m{\cdot}s^{-1}$. The observed maximum velocity among various debris flows events in Switzerland is 13 to 14 $m{\cdot}s^{-1}$ (Rickenmann and Zimmermann 1993).

The probable maximum runout was characterized by an average slope angle of 11° (Huggel *et al.* 2002). The average slope is the slope between the starting and end point following the debris flow path. So, we considered a constant friction loss corresponding to that angle, which results in a runout distance equal to the probable maximum runout (Figure 6).

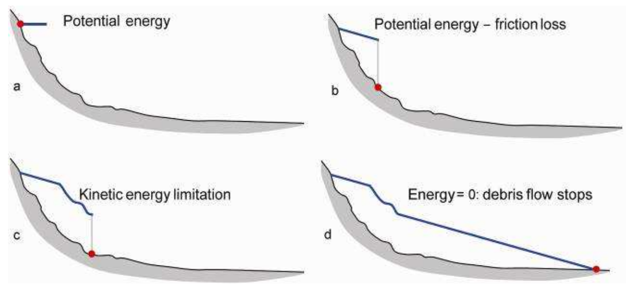

Figure 6: Illustration of the runout distance calculation principles (after Horton, 2008).

5.4 Results and comments

The results were based on the extreme events threshold for source areas identification. The obtained values correspond to the total area exposed to debris flow spreading with an associated qualitative probability qualifying the susceptibility, as shown in figure 7.
The color scale indicates the relative probability of propagation assuming that the sources possess the same probability of failure.

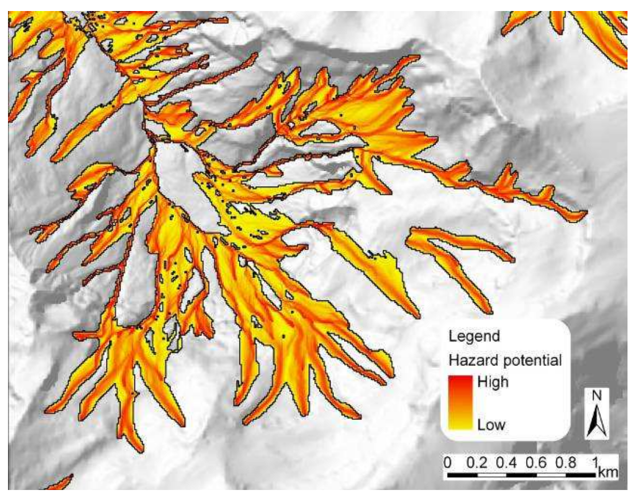

Figure 7: Spreading results for extreme events for the Les Diablerets (Switzerland) region, with representation of the probability values *(MNT-MO, © 2005 SIT).*

This present approach has its limits and does not reflect the local controlling factors and specific conditions. However, a good coherence between simulation results and field observations was obtained for specific catchments where major debris flow events have occurred. The proposed method demonstrates the efficiency of such a simplified approach.

6 ROCKFALL

The most difficult task for rockfall prediction is to define the potential rockfall source areas. Sources zones are usually taken from distinctive evidence (e.g. talus slope deposits below cliff faces, field measurements, and historical register information).

6.1 Identification of potential rockfall source area

Rocky outcrops and consequently unstable rockfall source areas are found in most cases in steep slopes. The slope processes are assumed to be controlled by rock type and slope gradient. As a consequence, the slope angle frequency distribution (histogram) of a given morphological unit varies randomly around its mean slope gradient (Strahler, 1954), which can be featured by Gaussian shape (Figure 8). Therefore, it is possible to decompose a histogram for a region located in a homogeneous geology in several different slope angle populations corresponding to each morphology such as cliffs and mountain sides. The maximum of the Gaussian distribution can be assumed as an apparent stable slope angle. In an alpine topography we encounter most frequently the following morphometric classes:

- Low slope gradients corresponding to the plains formed by fluvio-glacial deposits.
- Mid/gentle slope gradients corresponding to the lower part of the hillslope (Foothills & mountain flanks). They are characterized by alluvial fans (debris flow), landslide mass and till deposits.
- Steep slopes can be matched to the occurrence of rocky outcrops and cliff faces.

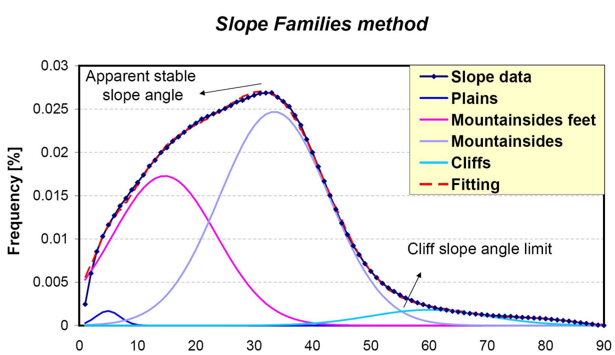

Figure 8: Slope angle frequency histogram featuring Gaussian populations (colored lines), where the peak of each curve represents the average slope of a distinctive morphology (after Loye et al, 2008).

The peak of each fitted curve reflects more precisely a distinctive threshold that can be correlated to major morphological units. In the present study the 1 m Lidar-DEM was used to perform the slope analysis, because of its accuracy.

6.2 Assessment of the maximum rockfall runout zones

Assessment of the runout zones from potential source areas described above was performed by means of the CONEFALL software (Jaboyedoff and Labiouse, 2003), which simply implements the cone method inspired from the shallow angle method (Toppe, 1987; Evans and Hungr, 1988) in a GIS environment. Thus, this GIS-based software allows the estimation of the maximum runout length in 3D by assuming a given aperture angle (90°- φ_p) centred on the source point (Figure 9). The cone method is empirical and doesn't require any other coefficient.

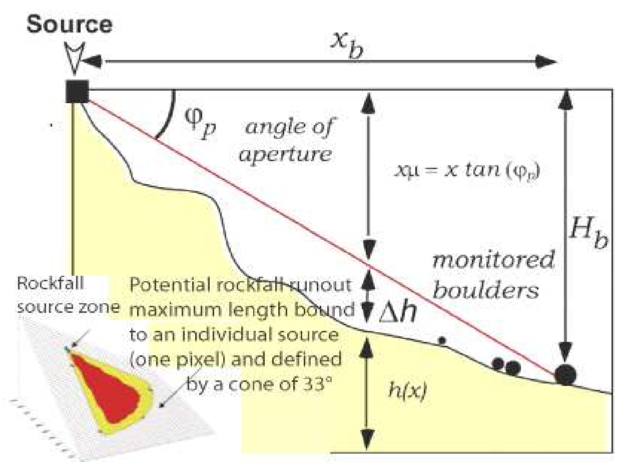

Figure 9: Scheme of the shadow angle method implemented in the GIS-based CONEFALL.

6.3 Data processing

The slope angle frequency histogram was performed on a DEM of 1m x 1m cell size (MNT-MO, © 2005 SIT). The canton of Vaud was divided into five study areas: The Helvetic, Ultrahelvetic and median Prealps gave three distinct slope angle frequency distributions of the Alpine topography. Plateau and Jura gave two others. For each of those five geologically-based units, a slope angle frequency distribution was computed and plotted. Rocky outcrops available from the 1:25,000 topographic vectorized map. steeper than the apparent stable slope angle, were considered as potential rockfall source areas. Then, Gaussian curves were fitted using an excel-based solver. Initial values were defined according to the shape of the slope angle histogram, where slope populations were obvious (unsteadiness in the distribution). Slope gradients steeper than the angle defined at the intersection between the estimated "Cliffs" and "Mountain sides" population were also considered as potential rockfall source areas, independently of the lithology and surface cover. This corresponds to the slope above which the "Cliffs" data distribution becomes dominant over the other morphometric classes ("Cliff" slope angle limit). Critical angles for each major unit are listed in Table 1. CONEFALL was applied to each potential source zone with an aperture angle of 33° for all units. This was established by comparison with rockfall events observed on orthophotos and fieldwork undertaken on test zones. The cone method performed over mountain sides that overhang alluvial plains models a maximum runout length too large compared to reality. A correction for the valley-bottom was therefore done to limit the runout length to 60 m.

In order to obtain a coherent document related to the cone method, the source data grid of 1 m x 1 m cell size was resampled to a 25 m x 25 m grid, because the cone method does not require such accuracy.

Table 1 : Threshold angles above which the rockfall source areas are potentially considered.

Tectonic unit	Threshold angle	
	Apparent stable slope angle	"Cliff" slope angle limit
Helvetic	36°	54°
Ultrahelvetic	33°	49°
Median Prealps	34°	53°
Molasse Basin (Plateau)	30°	46°
Jura Mountains	32°	46°

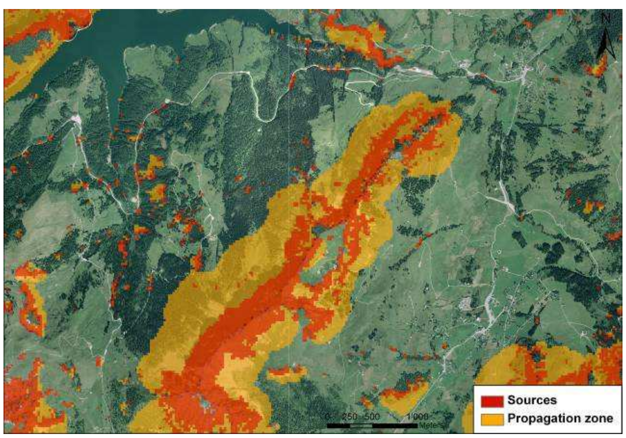

Figure 10: Close-up of the Indicative rockfall hazard map. Rockfall source zones are drawn in red and the runout perimeter in orange SWISSIMAGE © 2004 swisstopo (DV012716).

This cone method is a rather conservative way to consider cliff faces and slopes surfaces to be potentially instable over a certain slope gradient. Likewise, CONEFALL allows quick but accurate delineation of potential rockfall prone perimeters (Figure 10) and compares well with a 3D trajectography model, although it doesn't require physically-based parameters.

7 GENERAL CONCLUSION

Nowadays, the availability of LiDAR-DEM represents an important tool either to obtain a rapid overview of potential unstable areas or to perform more detailed studies as well. The methods introduced in this article show the potential of the DEM-based analysis for the more frequent types of slope mass movement susceptibility. These methods, relatively easy to use, allow a quick overview of the potential hazard affecting a large territory by using the best DEM data such as LIDAR-DEM. These results provide significant information of the zones where a more detailed analysis must be carried out for a complete hazard assessment. The quality of the results, however, depends on the DEM resolution and on the availability of other different spatial information.

8 REFERENCES

Ardizzone, F. Cardinali, M., Galli, M., Guzzetti, F., and P. Reichenbach 2007. Identification and mapping of recent rainfall-induced landslides using elevation data collected by airborne Lidar. Nat. Hazards Earth Syst. Sci., 7, pp. 637-650,

Claessens, L., Heuvelink, G.B.M., Schoorl, J.M. and Veldkamp, A. 2005. DEM resolution effects on shallow landslide hazard and soil redistribution modelling. Earth Surface Processes and Landforms, Vol. 30(4), pp. 461-477.

Delmonaco, G., Leoni, G., Margottini, C., Puglisi, C. and Spizzichino, D. 2003. Large scale debris-flow hazard assessment: a geotechnical approach and GIS modelling. Natural Hazards and Earth System Sciences, Vol. 3, pp. 443-455.

Erskine, R., Green, T., Ramirez, J. and MacDonald, L. 2006. Comparison of grid-based algorithms for computing upslope contributing area. Water Resources Research, Vol. 42(9).

Gamma, P. 2000. dfwalk-Ein Murgang-Simulationsprogramm zur Gefahrenzonierung. Geographisches Institut der Universität Bern.

Holmgren, P. 1994. Multiple flow direction algorithms for runoff modelling in grid based elevation models: An empirical evaluation. Hydrological Processes, Vol. 8(4), pp. 327-334.

Horton, P., Jaboyedoff, M., Bardou , E. (2008). Debris flow susceptibility mapping at a regional scale. In Locat, J., Perret, D., Turmel, D., Demers, D., and Leroueil, S., 2008. Proceedings of the 4th Canadian Conference on Geohazards. From Causes to Management. Presse de l'Université Laval, Québec, 594p.

Huggel, C., Kaab, A., Haeberli, W., Teysseire, P. and Paul, F. 2002. Remote sensing based assessment of hazards from glacier lake outbursts: a case study in the Swiss Alps. Canadian Geotechnical Journal, Vol. 39(2), pp. 316-330.

Hungr O. and Evans S. G, 1988. Engineering evaluation of fragmental rockfall hazard. Proceedings of the 5th International Symposium on Landslides, Lausanne, pp. 685-590.

Iverson, R.M. and Denlinger, R.P. 2001. Mechanics of debris flows and debris-laden flash floods, Seventh Federal Interagency Sedimentation Conference, Reno, Nevada.

Jaboyedoff, M. and Labiouse, V. 2003. Preliminary assessment of rockfall hazard based on GIS data. ISRM 2003 - Technology roadmap for rock mechanics, South African Institute of Mining and Metallurgy.

Lateltin, O., 1997. Recommandations - Prise en compte des dangers dus aux mouvements de terrain dans le cadre des activités de l'aménagement du territoire. Office fédéral de l'Environnement, des forêts et du paysage.

Loye, A., Pedrazzini, A., Jaboyedoff, M. 2008. Preliminary regional rockfall hazard mapping using LiDAR-based slope frequency distribution and Conefall modeling. In Locat, J., Perret, D., Turmel, D., Demers, D., and Leroueil, S., 2008. Proceedings of the 4th Canadian Conference on Geohazards. From Causes to Management. Presse de l'Université Laval, Québec, 594p.

Montgomery, D. R & Dietrich, W. E 1994. A physically-based model for the topographic control on shallow landsliding. Water resources Research, 30 1153-1171.

Noverraz F. - 1995 - Carte des instabilités de terrain du Canton de Vaud. Ecole Polytechnique Fédérale de Lausanne 33p.

Pack R., Tarboton & Goodwill, 1998. The SINMAP approach to terrain stability mapping. 8th congress of International Association of Engineering Geology, Vancouver.

Quinn, P., Beven, K., Chevallier, P. and Planchon, O. 1991. The prediction of hillslope flow paths for distributed hydrological modelling using digital terrain models. Hydrological Processes, Vol. 5(1), pp. 59-79.

Rickenmann, D. and Zimmermann, M. 1993. The 1987 debris flows in Switzerland: documentation and analysis. Geomorphology, Vol. 8(2-3), pp. 175-189.

Salciarini D., et al., 2006, Modeling regional initiation of rainfall-induced shallow landslide the eastern Umbria Region of central Italy, Landslide, 3, 181-194.

Strahler, A. N. 1954. Quantitative geomorphology of erosional landscapes. Compt. Rend. 19th Intern. Geol. Cong., Sec.13: pp. 341-354.

Tarboton, D.G. 1997. A new method for the determination of flow directions and upslope areas in grid digital elevation models. Water Resources Research, Vol. 33(2), pp. 309-319.

Toppe, R. 1987. Terrain models – a tool for natural hazard mapping. In Salm, B. and Gubler, H., editors, Avalanche formation, movement and effects. IAHS Publication no. 162, 629–38.

Trümpy, R., 1980. Geology of Switzerland—A Guide Book, Part A: An Outline of the Geology of Switzerland: Basel, Wepf & Co., 104 p.

Van Westen, C.J., Rengers, N., Terlien, M. et Soeters, R. 1997. Prediction of slope instability phenomena through GIS-based hazard zonation. Geol. Rundschau, 86, pp. 404-414.